Spatially Resolved Absorption Spectroscopy on a Microhollow Cathode Helium Plasma Using a Vertical-Cavity Surface-Emitting Laser*)

Kakeru TORII, Shota YAMAWAKI, Koichi KATAYAMA, Shinichi NAMBA[1], Keisuke FUJII,
Taiichi SHIKAMA and Masahiro HASUO

Graduate School of Engineering, Kyoto University, Katsura, Kyoto 615-8540, Japan
[1]*Graduate School of Engineering, Hiroshima University, 1-4-1 Kagamiyama, Higashi-Hiroshima,
Hiroshima 739-8527, Japan*

For the $1s2p(^1P) \rightarrow 1s3d(^1D)$ transition at 667.815 nm of helium in a microhollow cathode plasma with a 300 μm diameter, we measured the absorption spectra with spatial resolution of 30 μm using a vertical-cavity surface-emitting laser diode. The spectra observed near the electrode at 10 kPa gas pressure showed asymmetry. By analyzing the observed spectra with Voigt functions including the DC Stark effect, we evaluated the gas temperature, electron density, electric field strength and $1s2p(^1P)$ atom density and produced their two-dimensional maps.

© 2015 The Japan Society of Plasma Science and Nuclear Fusion Research

1. Introduction

Atmospheric-pressure plasmas have been attracting considerable attention because of their potential applications in surface treatment, nanoparticle formation and pollution gas processing, and so on [1]. Microhollow cathode discharge can generate such plasmas at moderate voltage. The gas temperature and electron density of the microhollow cathode plasma were measured with emission spectroscopy [2].

Compared with the emission spectroscopy, laser absorption spectroscopy is nearly free of spectral resolution; moreover, current modulation of the laser diode is often used because of its controllability. In atomic spectroscopy, a Fabry–Pérot laser diode and a distributed feedback laser diode have been used with typical mode-hop-free frequency scans of a few tens of GHz and several tens of GHz, respectively. However, at atmospheric pressure, the spectral line width is over several tens of GHz in full width at half maximum mainly because of the increase in the pressure broadening.

In this work, we used a vertical-cavity surface-emitting laser (VCSEL) diode to scan the light frequency over several hundreds of GHz in a single longitudinal mode [3, 4]. For the purpose of demonstrating the capability of VCSEL to characterize the plasma generated in a microhollow cathode with a 300-μm diameter, we measured the

absorption spectra associated with the helium $1s2p(^1P) \rightarrow 1s3d(^1D)$ transition and their spatial dependence. We show the results at gas pressure of 10 kPa, in which the spectral asymmetry owing to the sheath electric field is clearly observed and the plasma parameters are well evaluated.

2. Experiment

Figure 1 shows the microhollow cathode discharge generator. A 1-mm-thick ceramic insulator plate separates the 2-mm-thick cathode and 2-mm-thick anode, all of which have a discharge hole of diameter 300 μm in the center. The cathode and anode are made of stainless steel.
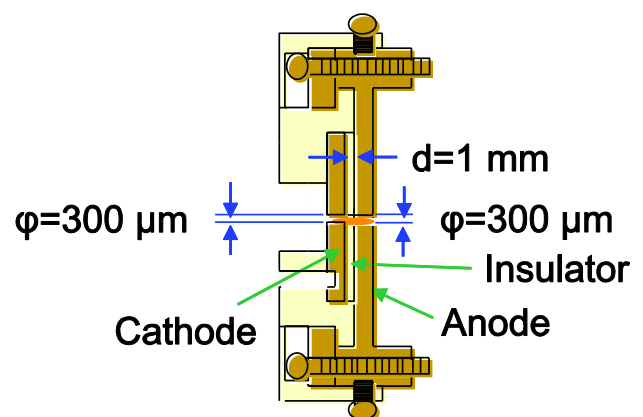
Fig. 1 Schematic of the microhollow cathode discharge generator.
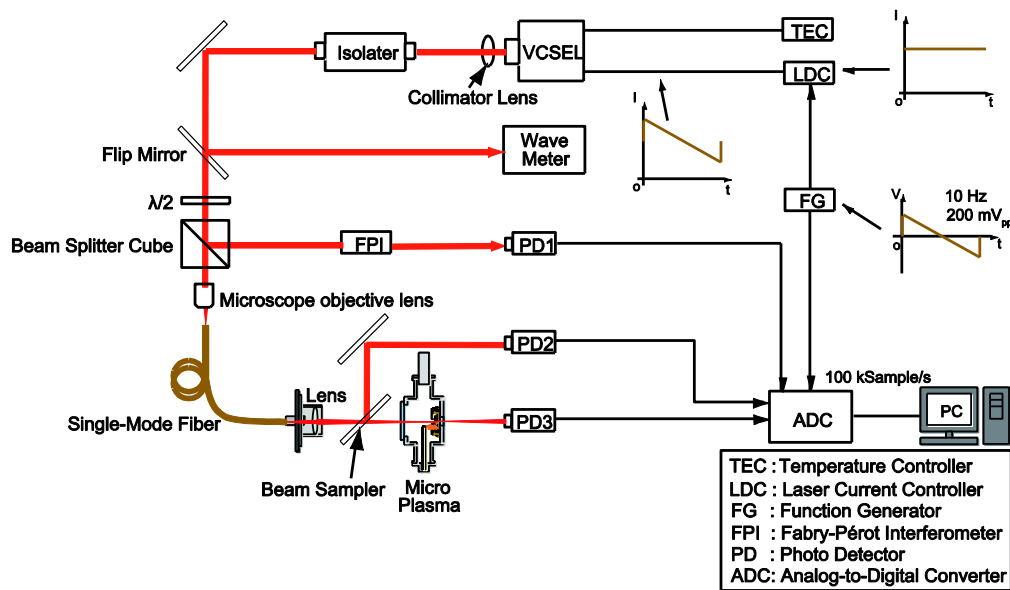
Fig. 2　Schematic of the experimental setup.

Figure 2 shows the experimental setup. The discharge chamber was evacuated to 0.4 Pa using a rotary pump (UL-VAC, GVD-050A) and then helium gas (99.999%) was introduced. The gas pressure was measured with an absolute digital pressure gauge (Valcom, VPMC-D-A-500kPa (abs)-1) and maintained at 10 kPa. The hollow cathode plasma was generated using a DC power supply (Takasago, GPO650-05R) with a ballast resistance of 20 kΩ. The discharge current was set at 15 mA and the output voltage from the DC power supply was about 540 V. The discharge chamber has observation windows on the cathode and anode sides.

The light source for measuring the absorption spectra was a VCSEL diode (Vixar, V670S-002-0001) positioned on a diode mount (Thorlabs, TCLDM9). The temperature of the laser diode was set at 4.01°C using a temperature controller (Profile, TED200). To scan the laser light frequency, we modulated the diode current by the voltage applied to the external input of a current controller (Thorlabs, LDC202C) from a function generator (Agilent, 33220A) at a scan time of 100 ms.

The collimated laser light beam passed through an optical isolator (Isowave, I-6070-CM). Before the measurement, we set the light frequency around that of the $1s2p(^1P) \rightarrow 1s3d(^1D)$ transition with a wavemeter (Burleigh, WA-4500D). Using a zeroth-order half-wave plate (Sigma Koki, WPQ-6943-2 M) and a polarized beam splitter (Thorlabs, PBS251), we divided the light beam into two; one was used in the frequency scan monitor using a Fabry–Pérot interferometer (Neoark, SA-40C; FSR = 1.98 GHz) with a photodetector (PD1) and the other in the absorption spectrum measurement. The second light beam was focused on the edge of a single-mode optical fiber. The optical fiber was used as a spatial filter to select the TEM$_{00}$ mode, which was confirmed by observing the

spatial pattern of the light transmitted through the optical fiber. We used a collimating lens to transform the transmitted light to a parallel beam of diameter about 3 mm. Then, we focused the parallel beam on the plasma with a 30 μm diameter in the Rayleigh criterion using a lens with a focal length of 150 mm. The diameter was measured by the knife-edge method. The increase in the diameter at 2 mm from the focal point was calculated at about 10 μm. We laterally tuned the focus position in the plasma by automatically tilting the focusing lens and measured the absorption spectrum with spatial steps of 10.8 μm. A similar spatially resolved absorption measurement has been performed for argon microplasma [5]. We confirmed that the tilt of the light beam in the plasma was negligible. Approximately a 2 μm lateral shift accompanied the 2 mm propagation. Part of the light beam was separated using a beam sampler (Suruga Seiki, F56-30) and the beam intensity was measured by a photodetector (PD2) as reference. The light intensity transmitted through the plasma was also measured using a photodetector (PD3). The outputs of the function generator and photodetectors PD1, PD2, and PD3 were recorded using an AD converter (National Instruments, USB-6251) and a personal computer.

3. Results and Discussion

Figure 3 shows an example of the raw data. The temporal evolutions of the function generator (a), PD2 (b), PD3 (c), and PD1 (d) outputs are shown. The sharp dip in Fig. 3 (c) is due to the $1s2p(^1P) \rightarrow 1s3d(^1D)$ transition in helium. Using the peaks in Fig. 3 (d), we convert the horizontal axis in Fig. 3 from scanning time to light frequency detuning. Note that the frequency scan range in Fig. 3 is over 500 GHz.

The light intensity measured with the PD3 is the sum
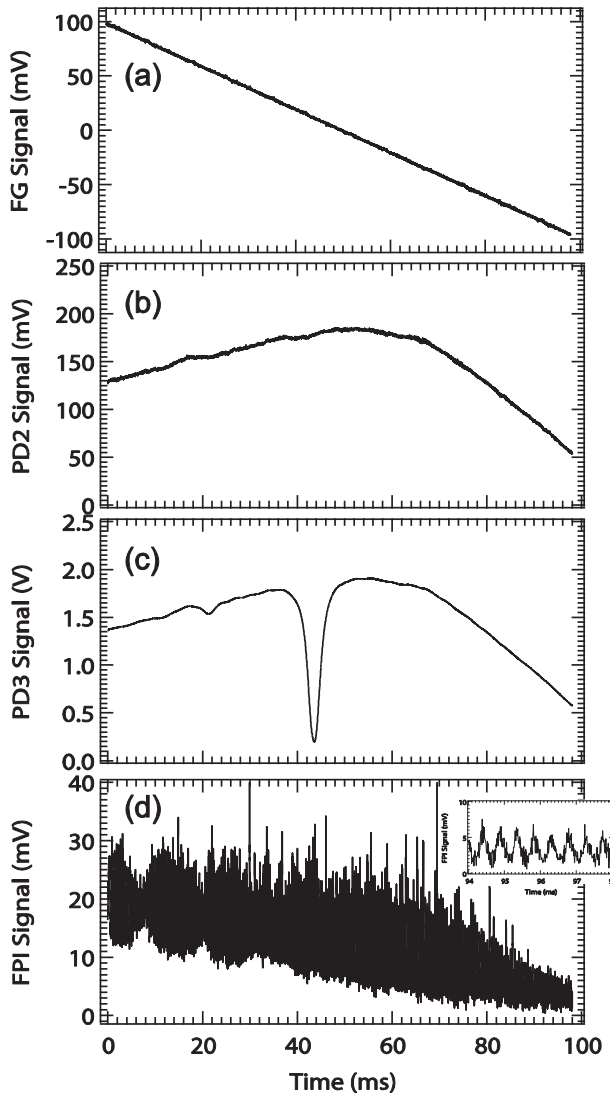
Fig. 3 Outputs of the function generator (a), PD2 (b), PD3 (c), and PD1 (d) as a function of the scanning time.

Fig. 4 Observed absorption spectra around the center (a) and around the edge (b) of the microhollow cathode plasma at 10 kPa. The fitting results are shown by the red curves.
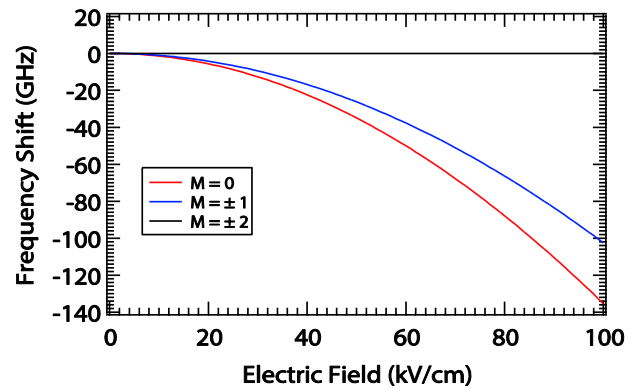
Fig. 5 Calculated frequency shift of the observed transitions by the second-order DC Stark effect. M is the magnetic quantum number of the helium atom 3^1D level.

of the laser light intensity I_t transmitted through the plasma and the plasma emission intensity. The plasma emission intensity is measured by cutting the laser light in front of the discharge chamber. On the other hand, the light intensity measured with the PD2 is proportional to the laser light intensity without the absorption I_0 by helium. Not only the sensitivies and gains of the PD2 and PD3 but also the intensities of the two light beams differed; thus, I_o and I_t were calibrated to coincide with each other in the frequency detuning region where helium absorption was absent. After the calibration, we calculated the absorption spectra using the following equation

$$\alpha(v)l = -\ln\left(\frac{I_t(v)}{I_0(v)}\right), \tag{1}$$

where $\alpha(v)$ is the absorption coefficient, v is the light frequency, and l is the light absorption length.

Figure 4 shows examples of the observed absorption spectra. The profile is symmetric (Fig. 4 (a)) at the center of the microhollow cathode plasma but asymmetric at the edge of the plasma, where a low-frequency tail is observed (Fig. 4 (b)).

It is known that there is a sheath electric field near the cathode [6] and the electric field leads to the Stark effect, which produces an asymmetric line profile or splitting [7]. We calculated the second-order Stark effect of the upper 3^1D level that dominates the observed transition line [7–9]. The result is shown in Fig. 5.

Without the Stark effect, the spectral profile is re-
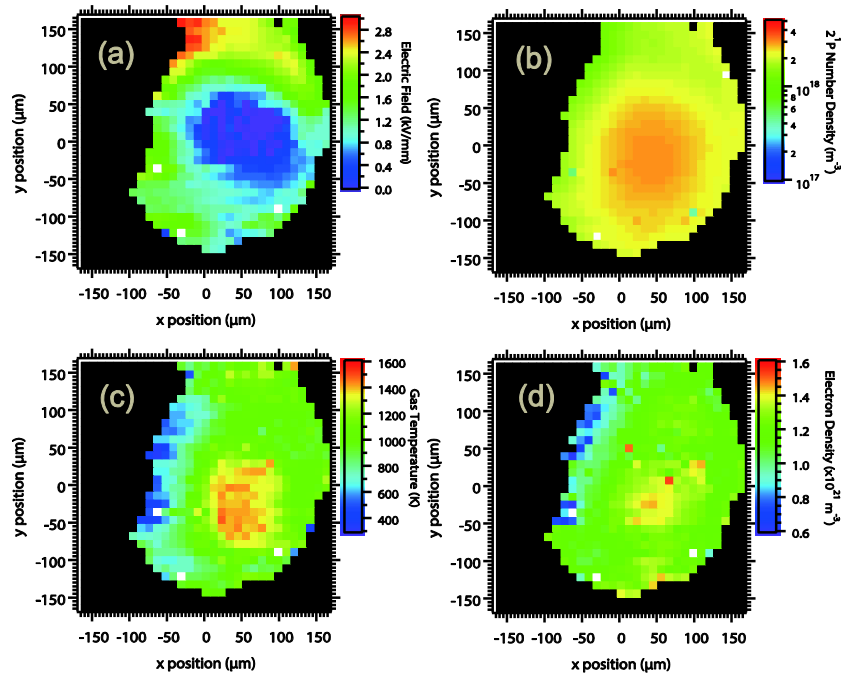
Fig. 6   Two-dimensional maps of the electric field strength (a), 2^1P atom density (b), gas temperature (c), and electron density (d) at 10 kPa based on the analysis of the spectra.

produced with a Voigt function, which is a convolution of Gauss and Lorentz functions. The Gauss and Lorentz functions reflect the Doppler and homogeneous broadening, respectively. Since it is found that a simple summation of the three Stark-splitting Voigt functions for the 3^1D level cannot reproduce the observed absorption spectrum, we treat the distribution of the electric field strength in the laser light spot using the first derivative of the electric filed strength as an adjustable parameter. Thus, the fitting function is

$$\alpha(v)l = -\ln\left[\frac{\int \frac{2I_0(v)}{\sqrt{2\pi}w_x}\exp\left\{-\frac{2x^2}{w_x^2} - \sum_M \alpha_M(v, E_{x=0} + \frac{\partial E}{\partial x}x)l\right\}\mathrm{d}x}{\int \frac{2I_0(v)}{\sqrt{2\pi}w_x}\exp\left(-\frac{2x^2}{w_x^2}\right)\mathrm{d}x}\right].$$
(2)

Here, w_x is the light beam radius where the light intensity is e^{-2} of the central intensity. x is the distance from the center of the laser light spot. $E_{x=0}$ is the electric field strength at the center of the laser light spot. α_M is the absorption coefficient for the 3^1D magnetic sublevels, where M is the magnetic quantum number.

Examples of the fitting are shown in Fig. 4. From this fit, we determined the Doppler and Lorentz widths as well as the electric field strength and its first derivative at the center of the laser light spot. From these widths, we evaluated the gas temperature and electron density using the gas temperature-dependent self-broadening coefficient [10] and the Stark broadening coefficient of 2.6×10^{-12} [$m^3 s^{-1}$] assuming an electron temperature of

2 eV [11]. We also evaluated the lower 2^1P atom density n_{2P} from the absorption spectrum as [5, 12]

$$n_{2P} = \frac{4\varepsilon_0 m_e c}{e^2 f_a l}\int \alpha(v)l\mathrm{d}v,$$
(3)

where ε_0 and c are the dielectric constant and speed of light in vacuum and m_e and e are the electron mass and elementally charge, respectively, and f_a is the absorption oscillator strength of the 1s2p(^{1}P) $\rightarrow$ 1s3d(^{1}D) transition. In the evaluation, we assumed $l = 4$ mm from the thickness of the electrodes.

Figures 6 (a), 6 (b), 6 (c), and 6 (d) show two-dimensional maps of the evaluated electric field strength, 2^1P atom density, and gas temperature and electron density, respectively, at 10 kPa. The electric field strength and the line-integrated value of its first derivative differ by a factor of two at most. The observed spatial distributions of the 2^1P atom density, gas temperature, and electron density peak around the plasma center. On the other hand, the electric field strength is high near the electrode. The distribution of the field strength does not have rotational symmetry. The lack of rotational symmetry may be due to the roundness imperfections and surface roughness of the electrode.

4. Conclusion

We observed the spatially resolved absorption spectra of the helium 1s2p(^{1}P) $\rightarrow$ 1s3d(^{1}D) transition line in microhollow cathode helium plasma. From the analysis of the observed spectra, we evaluated the two-dimensional distri-

butions of the electric field strength, 2^1P atom density, gas temperature, and electron density at 10 kPa.

[1] D. Mariotti and R.M. Sankaran, J. Phys. D: Appl. Phys. **44**, 174023 (2011).
[2] S. Namba, T. Yamasaki, Y. Hane, D. Fukuhara *et al.*, J. Appl. Phys. **110**, 073307 (2011).
[3] J. Wang, S.T. Sanders, J.B. Jeffries and R.K. Hanson, Appl. Phys. B **72**, 865 (2001).
[4] S.T. Sanders, J. Wang, J.B. Jeffries and R.K. Hanson, Appl. Opt. **40**, 4404 (2001).
[5] N. Miura and J. Hopwood, J. Appl. Phys. **109**, 013304 (2011).
[6] M.J. Kushner, J. Phys. D: Appl. Phys. **38**, 1633 (2005).
[7] T. Fujimoto, *Plasma Spectroscopy* (Clarendon press, Oxford, 2004).
[8] W.L. Wiese and J.R. Fuhr, J. Phys. Chem. Ref. Data **38**, 565 (2009).
[9] A.G. Frank, V.P. Gavrilenko, N.P. Kyrie and E. Oks, J. Phys. B: At. Mol. Opt. Phys. **39**, 5119 (2006).
[10] A. Atiola, B.C. Gibson-Wilde, A.C. Lindsay *et al.*, J. Phys. B: At. Mol. Opt. Phys. **21**, 249 (1988).
[11] H.R. Griem, *Plasma Spectroscopy* (McGraw-Hill, New York, 1964).
[12] A. Thorne, U. Litzen and S. Johansson, *Spectrophysics Principles and Applications* (Springer, 1999).